Axisymmetric Hurricane in a Dry Atmosphere: Theoretical Framework and Numerical Experiments

AGNIESZKA A. MROWIEC

Columbia University, New York, New York

STEPHEN T. GARNER

GFDL, Princeton, New Jersey

OLIVIER M. PAULUIS

New York University, New York, New York

(Manuscript received 11 August 2010, in final form 10 March 2011)

ABSTRACT

This paper discusses the possible existence of hurricanes in an atmosphere without water vapor and analyzes the dynamic and thermodynamic structures of simulated hurricane-like storms in moist and dry environments. It is first shown that the ''potential intensity'' theory for axisymmetric hurricanes is directly applicable to the maintenance of a balanced vortex sustained by a combination of surface energy and momentum flux, even in the absence of water vapor. This theoretical insight is confirmed by simulations with a high-resolution numerical model. The same model is then used to compare dry and moist hurricanes. While it is found that both types of storms exhibit many similarities and fit well within the theoretical framework, there are several differences, most notably in the storm inflow and in the relationship between hurricane size and intensity. Such differences indicate that while water vapor is not necessary for the maintenance of hurricane-like vortices, moist processes directly affect the structure of these storms.

1. Introduction

Intertwining dynamics and thermodynamics across scales ranging from 10 m to 1000 km, hurricanes are arguably the most complex type of coherent structure found in the earth's atmosphere. Not surprisingly, a unified theory for their intensity, scale, and variability is still elusive. Here we propose an approach based on the suppression of one of the most complex components of hurricane dynamics: water vapor. Specifically, we show that the theoretical framework of Emanuel (1986, hereafter E86) is applicable to the maintenance of axisymmetric hurricanes in the absence of water vapor, and we confirm such predictions in a numerical model.

There have been a number of theoretical attempts to devise a single variable that would quantify hurricane strength and also be predictable. From all of the theories, there emerge two major groups: one group assumes that the sources of hurricane energy are the air–sea interaction and the thermodynamic disequilibrium between the atmosphere and ocean (Kleinschmidt 1951; E86; Emanuel 1995; Pearce 1998, 2004), while the other supposes that the main energy source is the convective available potential energy (CAPE) (Miller 1958; Malkus 1958; Malkus and Riehl 1960; Holland 1997).

The work presented here is guided by the potential intensity (PI) theory of E86. This theory combines the thermodynamics of a hurricane with the dynamics of its circulation through the angular momentum M and entropy S relationship. The assumptions of slantwise moist neutrality and gradient wind balance lead to a dynamically and thermodynamically constrained vortex. Emanuel introduced the wind-induced surface heat exchange (WISHE) mechanism, which assumes that a tropical storm can gain energy through a positive feedback between the wind speed and the surface fluxes. He also argued that the CAPE has little to do with

Corresponding author address: Agnieszka A. Smith-Mrowiec, NASA Goddard Institute for Space Studies, 2880 Broadway, New York, NY 10025.
E-mail: asmithmrowiec@giss.nasa.gov

DOI: 10.1175/2011JAS3639.1

© 2011 American Meteorological Society

hurricane intensification: if ambient CAPE is present, a hurricane can use it, but it is not the primary energy source for tropical storms. The idea of a CAPE energy source is not borne out by models and observations.

Slantwise moist neutrality and thermal wind balance enable a direct analytical relationship among entropy, angular momentum, and the tangential wind. The maximum tangential wind expression developed in a series of theoretical PI papers (E86; Emanuel 1988b, 1995) is sensitive to the relative humidity under the eyewall, the tropopause temperature, and the sea surface temperature, but also the air–sea exchange coefficients (for both heat and momentum). The original theory of E86 describes how the intensification and maintenance of tropical cyclones depends solely on self-induced heat transfer from the ocean and gives an upper limit on the intensity. This theory predicts that the structure of a mature hurricane is mainly determined by the entropy and angular momentum distributions in the boundary layer, which are set by surface fluxes (the dependence of outflow temperature on entropy could also potentially influence the structure of the vortex).

Hurricanes in the earth's atmosphere are sustained by a combination of latent and sensible heat fluxes from the ocean. In the dry case, only sensible heat flux is present, but if the absence of the latent energy source is compensated through an enhancement of the sensible heat flux, we show here that the PI theory still applies. Using a nonhydrostatic, axisymmetric numerical model, we further demonstrate here that a stable hurricane-like storm can be maintained in the absence of water vapor. We analyze the general properties of dry storms and contrast them with simulations of moist hurricanes with the same model. Finally, we analyze the sensitivity of the modeled storms to initial conditions and compare dry hurricanes in steady state with moist storms produced in similar environmental conditions.

2. Review of the axisymmetric theory

The PI theory (E86; Emanuel 1988a, 1995) offers a dynamically and thermodynamically consistent framework to predict the maximum possible hurricane intensity. The theory considers the maintenance of a steady axisymmetric vortex that is sustained by surface energy and momentum fluxes. The theory rests on two sets of assumptions. First, a set of dynamical balance assumptions is used to determine the structure of the storm within the free troposphere according to a given distribution of entropy and angular momentum in the boundary layer. The second set of assumptions is related to the energy and angular momentum budget of the boundary layer, and these lead to a closure for the entropy and angular momentum distributions as a function of surface exchange coefficients and the thermodynamic disequilibrium between the atmosphere and ocean. We argue that this theoretical framework is equally applicable to dry and moist atmospheres. A review of the potential intensity theory follows below.

a. Maximum wind equation

E86 assumes slantwise moist neutrality, gradient-wind balance, hydrostatic balance, and axisymmetry. Slantwise neutrality means that, above the boundary layer, saturated moist entropy lines are also constant angular momentum lines, and this implies frictionless outflow and conservation of moist entropy. Neutrality to slantwise convection, together with gradient wind and hydrostatic balance, enables simple analytical relationships among entropy, angular momentum, and tangential wind. The original formulation neglects turbulent mixing in the boundary layer, assuming it to be small in comparison with the major energy source of the storm.

Gradient wind balance can be expressed as $V^2/r + fV = g\partial z/\partial r|_p$, where V is the tangential wind, r is the radius, g is the gravitational acceleration, f is the Coriolis parameter, and p is the pressure. With the aid of hydrostatic balance, this can be rewritten in terms of angular momentum,

$$M = rV + \frac{1}{2}fr^2, \tag{2.1}$$

leading to the thermal wind equation [(6) in E86]

$$\frac{1}{r^3}\frac{\partial M^2}{\partial p}\bigg|_r = -\frac{\partial \alpha}{\partial r}\bigg|_p, \tag{2.2}$$

where $\alpha = \rho^{-1}$ is the specific volume of air.

Notice that there is no explicit mention of moisture in (2.2): in the dry system, changes of density are, without approximation, related directly to changes in entropy. By contrast, the equation of state for moist air indicates that density is a function of pressure, entropy, and total water. In particular, the effects of water content on density are not always negligible (Stevens 2005). The original PI theory of E86 neglected the effects of moisture on specific volume, but these were subsequently added to the PI theory in Emanuel (1988a). We emphasize that the dry framework used here is not intended to be a substitute theory for moist dynamics, but rather a theoretical tool used to understand the dynamics of hurricanes in a simplified but thermodynamically consistent framework.

The use of the Maxwell relation $(\partial\alpha/\partial S)|_p = (\partial T/\partial p)|_S$ converts thermal wind balance [(2.2)] to a formula for

the slope of the outflow M (or S) surfaces (see E86 for details), namely

$$\left.\frac{dr}{dp}\right|_M = \frac{r^3}{2M}\frac{dS}{dM}\left.\frac{\partial T}{\partial p}\right|_S, \tag{2.3}$$

where $dM = \partial M/\partial r|_p\, dr + \partial M/\partial p|_r\, dp$ is calculated on constant M surfaces. This equation can be integrated from the top of the boundary layer under the eyewall to the outflow pressure level, resulting in an expression for the outflow surfaces. Thus, the entire structure of the storm is determined once the distribution of dS/dM is known at the top of the boundary layer. When the outflow region is far from the center of the storm, the integral of (2.3) may be written as [(11) in E86]

$$r^2|_M = -\frac{M}{(dS/dM)\Delta T}, \tag{2.4}$$

where $\Delta T = T - T_o$ and T is the temperature at top of the boundary layer in the eyewall while T_o is the outflow temperature. Finally, when this result is considered within the eyewall of a hurricane, and the angular momentum is approximated as $M \approx rV$, the relationship among the hurricane intensity, the derivative of the entropy with respect to the angular momentum, and the outflow temperature becomes

$$V^2|_M = -M\frac{dS}{dM}\Delta T. \tag{2.5}$$

Thus, strong tangential winds are associated with strong gradients of entropy with respect to angular momentum.

b. Boundary layer closure

The relationship between the maximum tangential wind and rates of change of entropy and angular momentum [(2.5)] is not sufficient to predict the velocity because the factors controlling the distribution of entropy and angular momentum near the surface are not determined. E86 proposes a semiempirical boundary layer horizontal structure composed of three well-mixed regions: the eye of the storm (region I) ranging from the storm's center to the inner side of the eyewall, the eyewall (region II) from its innermost radius to the radius of maximum wind (RMW), and the region from the RMW to the outer edge of the hurricane (region III). The S–M relationship is described by a balance between the entropy gain during the inflow and the loss of angular momentum due to friction. The eye does not actively participate in the dynamics and the dissipative heating in the boundary layer is excluded.

Under turbulent conditions, mean values of S and M are conserved and assumed to be well mixed in the boundary layer, and vary following the mean radial motion according to

$$\frac{dS}{dt} = -\frac{1}{\rho}\frac{\partial \boldsymbol{\tau}_S}{\partial z},$$

$$\frac{dM}{dt} = -\frac{1}{\rho}\frac{\partial \boldsymbol{\tau}_M}{\partial z}, \tag{2.6}$$

where $\boldsymbol{\tau}_S$ is the vertical heat flux and $\boldsymbol{\tau}_M$ is the vertical angular momentum flux. These fluxes are produced by all processes excluding the mean storm circulation. If a steady state is assumed and the entropy is solely a function of angular momentum, then $dS/dt = (dS/dM)(dM/dt)$. In Emanuel's middle region, the fluxes at the top of the boundary layer are assumed to be negligible: only the surface fluxes are used to determine the entropy and angular momentum distribution:

$$\left.\frac{dS}{dM}\right|_h = \left.\frac{\boldsymbol{\tau}_S}{\boldsymbol{\tau}_M}\right|_0. \tag{2.7}$$

The surface fluxes over the ocean are given by standard aerodynamic formulas:

$$\boldsymbol{\tau}_S = -c_k|\mathbf{V}|\Delta S \tag{2.8}$$

$$\boldsymbol{\tau}_M = -c_d|\mathbf{V}|Vr, \tag{2.9}$$

where $\Delta S = S - S_s$, with S_s being a value of entropy of air that is in a thermodynamic equilibrium with the sea surface and S the entropy at the top of the boundary layer. The parameters c_k and c_d are the exchange coefficients for the entropy and the angular momentum, respectively. Using (2.7)–(2.9) and incorporating the V^2 relation [(2.5)] leads to the closed hurricane intensity equation:

$$V^2 = -\frac{c_k}{c_d}\Delta S \Delta T. \tag{2.10}$$

This statement gives the maximum tangential wind determined by the thermodynamic disequilibrium at the surface under the eyewall and by the temperature at the outflow level.

c. Dry framework

As in the original PI theory, the dry theoretical framework adopted in this paper uses hydrostatic and gradient wind balance to establish the relationship between the tangential wind and S–M distribution. E86 introduces moisture implicitly, through its effects on the entropy:

$$S_m \approx c_p \ln\theta + \frac{L_v q}{T}, \tag{2.11}$$

where θ is the potential temperature and L_v is latent heat of vaporization. The first term in (2.11) is directly affected by sensible heating and the second term by the latent heating. In a dry framework the latent heating is absent and the dry entropy is

$$S_d = c_p \ln\theta. \tag{2.12}$$

Surface fluxes increase the entropy and decrease the angular momentum of the inflowing air. In doing so they determine the entire structure of the balanced vortex. In the PI theory, water vapor is only relevant through its impact on entropy, so if the same entropy increase were produced through an increase in temperature and not in the humidity, we would expect similar overall behavior from the storms developed in both thermodynamic regimes.

3. Details of the numerical model

a. Model physics

In the study presented here we used an axisymmetric, nonhydrostatic version of the Geophysical Fluid Dynamics Laboratory (GFDL) regional atmospheric model. Developed by S. Garner, C. Kerr, O. Pauluis, and I. Orlanski, the model is designed for compressible atmospheric flow simulations (see, e.g., Pauluis and Garner 2006). The physical parameterizations used in our setup include Monin–Obhukov similarity theory (Garatt 1992) for the surface fluxes and a turbulent kinetic energy (TKE) scheme for interior mixing (Klemp and Wilhelmson 1978). The latter is applied to the wind fields, temperature fields, and moisture fields (if applicable). In the Monin–Obukhov scheme, the surface roughness calculation incorporates a diagnosis of wave heights according to Beljaars (1994) or Moon et al. (2006). Radiation is calculated with the GFDL radiation package (Anderson et al. 2004), in which the shortwave radiation algorithm follows Freidenreich and Ramaswamy (1999) and the longwave radiation is based on a simplified exchange approximation (Schwarzkopf and Ramaswamy 1999). For both shortwave and longwave radiation, water vapor (where applicable) is parameterized by the Clough–Kneizys–Davies 2.1 formulation, as described in Clough et al. (1992). In the dry experiments moisture does not enter the radiation package.

No parameterization for either shallow or deep convection has been used. The high model resolution allows for convection to be resolved. In the moist experiments, the bulk microphysical parameterization of Lin et al. (1983), with modifications proposed by (Lord et al. (1984) and Krueger et al. (1995), is used. In the dry framework bulk microphysics effects, surface evaporation, and saturation vapor pressure are set to zero.

b. Boundary conditions

The model is configured for axisymmetric hurricanes, with a wall at the inner boundary. At the outer boundary, the horizontal velocities are nudged to zero and the temperature and humidity (when applicable) are nudged toward environmental reference conditions. The nudging is applied over the outer 50 km to allow for the free evolution of the hurricane with minimal forcing near the eye. At the top boundary, to minimize the reflection of small-scale inertia–gravity waves, we apply an energy-absorbing sponge, in the form of gradual Newtonian damping to a running mean of the evolving fields, applied over the top 4 km.

Surface temperature at the bottom boundary is constant and set to 300 K in (we also tested other values of surface temperature). Our strategy was to use similar surface temperatures in the dry and moist experiments. The difference between the temperature at the surface and the lowest atmospheric level is set to 10 K in the control experiment with the dry model. This temperature jump is a crucial control parameter: it ensures that the developing storm has an enhanced energy source in the absence of a latent heat source. For hurricane surface inflow ($z = 0$) at constant temperature of 300 K, an air–sea temperature contrast of about 2 K, with relative humidity in the environment of about 85% and under the eyewall of about 95%, a straightforward calculation of moist static energy gain gives $\Delta h_m = c_p \Delta T_m + L_v \Delta r_v \approx 10^4$ J kg^{-1}. In the dry framework the same gain in dry static energy, $h_d = c_p \Delta T_d$, yields a temperature disequilibrium of about 10 K. We tested a case where the temperature at the surface was equal to that of the atmosphere and under such conditions the storm did not develop. We also ran experiments for temperature differences of 5 and 20 K. In the former case the observed storm took longer to reach a steady state, and the resulting vortex was slightly weaker and wider than for a 10-K temperature difference. In the latter case the storm was more intense, with a smaller eye.

In the dry experiments, the environmental temperature profile is given by a dry adiabat within the troposphere, consistent with the notion that the environment is in radiative–convective equilibrium, and stably stratified above the tropopause. For the standard dry run, the imposed disequilibrium of 10 K means that the reference potential temperature is $\theta = 290$ K within the troposphere. The tropopause is marked by an increase of the lapse rate of potential temperature to 17 K km^{-1} at about 10 km in the control run. The tropopause

height is one of the control parameters for dry the numerical simulations, and it can be easily modified for various experiments.

Numerical convergence was tested by comparing simulations for the same physical initial conditions but with four different horizontal resolutions. Values of the resulting maximum tangential wind for the steady hurricane, time averaged over 72 h, were 66, 67, 76, and 76.5 m s^{-1}, respectively, for resolutions of 2 km, 1 km, 500 m, and 250 m. The 2-km resolution result is smoother compared to the higher-resolution runs, and it also has the lowest maximum tangential wind. All but the 2-km run reached steady state in about 7 days. The lowest-resolution run takes about 50 h longer to achieve its steady state, and the transient evolution is quite different. Based on these observations, we used 1-km or 500-m horizontal resolution in our experiments.

The moist simulations were initialized similarly to the dry runs, with assigned values of surface temperature. The humidity and temperature profiles, compiled by Jordan (1958) for mean summer conditions over the Caribbean, were used for the environmental profiles. One of the features of this profile is a relatively high value of equivalent potential temperature θ_e in the planetary boundary layer, and a sharp decrease of θ_e with height.

c. Initialization and spinup

The main experiments presented here were run in a 5° domain with 1-km and 500-m horizontal resolutions, and constant f corresponding to a latitude of 15°N. The model has a stretched vertical coordinate, with 40 vertical levels and the topmost level at 23.5 km. We also tested a larger domain (10°), other horizontal resolutions (2 km and 250 m), and two other f values (5° and 30°). Simulations were run up to 30 days, even though the steady state is reached much sooner.

All hurricane runs were initialized with a weak, bottom-intensified vortex with 5 m s^{-1} tangential wind, located at approximately 100 km from the origin. This initial disturbance is not sustained and dissipates quickly; however, it establishes a weak surface frictional convergence that contributes to ascent and initiates convection. The relative vorticity of the initial disturbance is about $10f$. As pointed out by Gray (1968), initial disturbances with nonzero relative vorticity are crucial for hurricane development. However, we suspect that the geometry of this model makes this detail less important. We tested the sensitivity of the mature storm's intensity to the strength and location of the initial disturbance and found that they had no significant influence on the resulting steady storm. However, we ran a case with no initial disturbance and found that a storm in this case did not develop. We also initialized a storm at the equator ($f = 0$) and observed no storm development.

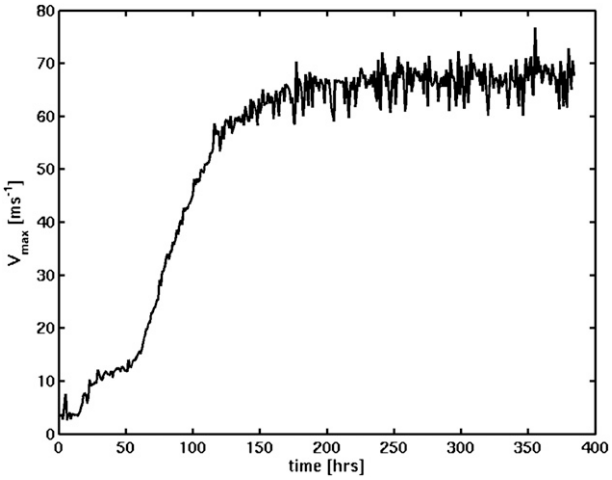

FIG. 1. Time evolution of the maximum wind in a dry storm. The vortex intensification starts after about 70 h and within the next 2 days the maximum tangential wind increases from about 18 to over 60 m s^{-1}. After about 150–200 h the storm reaches the statistically steady state.

An example of dry storm development is presented in Figs. 1 and 2 (note that time in Fig. 2 runs from top to bottom). For this case, the domain size is 550 km, the horizontal resolution is 1 km, the environmental profile is given by the dry adiabat prescribed in the troposphere, the surface temperature is 300 K, the Coriolis parameter is 3.7×10^{-5} s^{-1}, and the air–surface temperature contrast is 10 K. The initial vortex dissipates quickly, within the first 50 h. The steady storm forms from the frontlike inflow, which intensifies as it approaches the center of the domain. This is consistent with Emanuel (1997), who demonstrates that the frontogenetic nature of the hurricane eyewall is an important factor in storm evolution.

The major intensification starts after about 70 h (Fig. 1). Over the next 2 days the storm spins up from about 18 m s^{-1} to over 60 m s^{-1}. After about 150–200 h the storm reaches its maximum intensity and becomes a statistically steady warm-core vortex. The rapid intensification is associated with a moving front (Fig. 2), which forms the boundary of a strong inflow of low-level air. Note the intensification of the tangential wind as the front moves and tightens the vortex. The process by which the dry vortex reaches the statistically steady state (starting off far away from the initial vortex) may not be what is usually expected in realistic situations.

Similarly to dry runs, the moist experiments take about 120–150 h to fully spin up (not shown). In the moist systems the environmental reference state is crucial and can bring quite large variability into the spinup

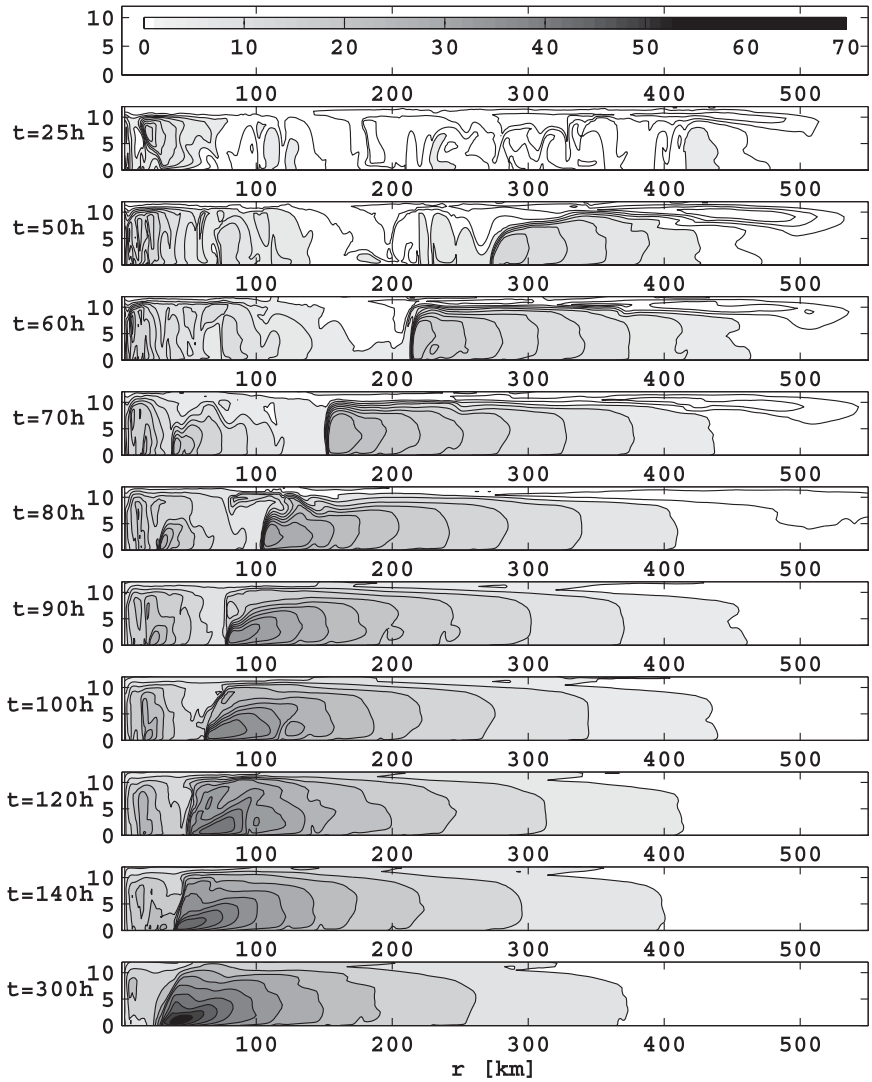

FIG. 2. The intensification of a dry hurricane has a frontal structure seen here in snapshots of tangential wind contours (m s^{-1}). Time increases from top to bottom. Vertical axes mark height (km) and extend to 12 km. Note the increasing intensity as the front comes closer to the center of the vortex.

process. We do not discuss the details of moist spinup since the main focus here is on the maintenance of the dry storm.

4. Steady-state dry and moist hurricanes

Although modeled storms become steady after about a week, the simulations were extended beyond that time for the purpose of time averaging, which is done to remove the high-frequency fluctuations. The time averaging was done over a subjectively chosen 72-h interval during the quasi-steady period. Figure 3 shows the time-mean tangential, radial, and vertical wind in the dry case run on the 5° domain with 500-m resolution and 300-K surface temperature. The time-averaged tangential wind, plotted in Fig. 3a, has a maximum intensity of about 67 m s^{-1}, located at a radius of 36 km (the RMW) and at a height of approximately 800 m. The circulation is cyclonic everywhere except for the high-altitude region far away from the center, where it becomes anticyclonic. The top branch of the secondary circulation may be thought of as a region corresponding to the outflow in the theory.

Figure 3b shows the radial velocity. The intensity of the dry inflow jet near the surface increases rapidly at about 100 km from the center and reaches a maximum of 20 m s^{-1} at about 60 km. The inflow jet maximum is confined below 5 km and it collapses near the RMW.

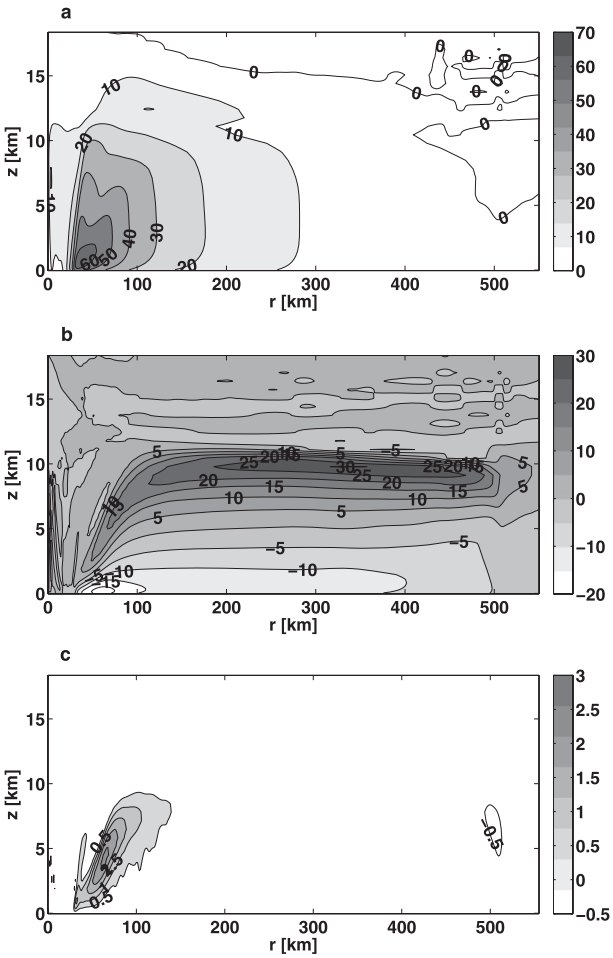

FIG. 3. Contour plots of the cross sections of the quasi-steady-state velocity fields (m s^{-1}) in a dry vortex averaged over 72 h, showing (a) tangential wind, (b) radial wind, and (c) vertical wind. The surface temperature in this case was 300 K, with 500-m resolution.

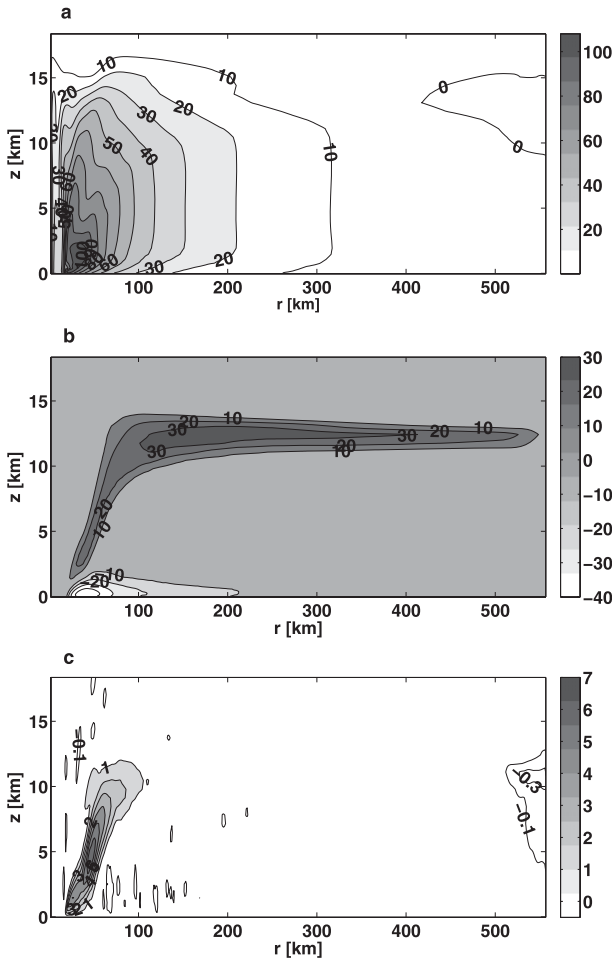

FIG. 4. Quasi-steady-state velocity fields (m s^{-1}), averaged over 72 h, simulated with Lin microphysics, the Jordan environmental profile, 300-K surface temperature, and 500-m horizontal resolution, showing (a) tangential wind, (b) radial wind, and (c) vertical wind. Note that the range of the grayscale is different than in Fig. 3.

The outflow does not exhibit such sharp horizontal gradients: it reaches its maximum immediately below the tropopause (at about 10 km) and is located at about 340 km from the center.

The time-averaged vertical velocity is shown in Fig. 3c. The updraft maximum is located above the height of the maximum tangential wind, which is typical for both modeled and observed tropical storms. The ascending air closely follows isentropic surfaces (not shown), corresponding here to surfaces of constant potential temperature. As can be seen in Fig. 3c, convection is not upright but flares out with height. At the location of maximum convergence the inflow is forced to change its direction and the air is convected upward, and finally away in the outflow at the tropopause.

A typical storm wind field time-averaged over 72 h for the moist case is shown in Fig. 4. The case described here was run with Lin microphysics, the Jordan environmental profile, 300-K surface temperature, and 500-m horizontal resolution. Figure 4a shows the tangential wind field. For this experiment a steady-state maximum wind of about 105 m s^{-1} is located at a radius of about 25 km.

In Fig. 4b the radial wind field is shown. The maximum inflow velocity is located outside and below of the location the maximum tangential wind. The maximum inflow speed near the eyewall is about 40 m s^{-1}. Outflow at the tropopause is stretched over a longer distance as compared to inflow and reaches a maximum value of 30 m s^{-1}. Unlike the tangential wind, the radial wind has considerably different character in the dry and moist regimes. In the dry case, the strong inflow and outflow jets have similar thickness outside the eyewall. In the moist simulations, the outflow dominates the upper portion of the domain. The strong inflow is limited to a narrow boundary layer near the surface, and contrasts

markedly with the much deeper inflow in the dry simulations. This difference can be attributed the fact that, while the moist boundary layer can be stabilized by subsidence in the free troposphere above it, the environmental profile for the dry run has a uniform potential temperature, which prohibits the formation of a capping inversion. The strength of both dry and moist secondary circulations is comparable, but the location of the maxima is not. The moist outflow maximum is located closer to the eyewall than the dry one. This difference between the strong inflow and the outflow depth is most likely caused by the presence of the convective downdrafts that limit the inflow boundary layer extent.

Figure 4c shows the vertical velocity of the moist hurricane in steady state. The main branch of the updraft in the eyewall has a quite similar structure for both dry and moist thermodynamics, but it is stronger in the moist case (6 m s^{-1}) than in the dry case (2.5 m s^{-1}). The greater vertical extent of the moist vortex is related to the environmental profile and the location of tropopause. For moist storms the outflow is located at a height of 12 km and for the dry vortex it was imposed at 10 km. There is less convective activity in the eye of the storm and, unlike the dry case, there are many downdrafts on the outside of the eyewall. The dry, time-mean vertical velocity is almost zero everywhere except at the outer edge of the domain, where it was forced to descend (Fig. 3c). In the moist case, the downdrafts are numerous, and the strongest of them are located right on the outer edge of the eyewall. This difference is a strictly moist effect and maintains the environmental midlevel minimum in the entropy and equivalent potential temperature.

The structure of the quasi-steady dry entropy and angular momentum fields is shown in Fig. 5. High angular momentum (Fig. 5a) is advected from the outer regions toward the eyewall by the hurricane inflow. Part of the angular momentum is dissipated during inflow due to friction at the surface. Throughout much of the domain above the boundary layer the angular momentum is well mixed and exhibits a strong horizontal gradient within the eyewall. According to the theoretical assumption of neutrality to slantwise convection, the entropy and angular momentum lines should have the same slope within the eyewall region and, to a first approximation, they do.

The largest values of entropy found anywhere in the lower troposphere occur in the hurricane eye. There are two regions within the dry storm in which the entropy is well mixed vertically: the eye of the hurricane, and the region outside of the eyewall (Emanuel's regions I and III, respectively). In the latter, the lowest values of entropy are mixed up from the surface all the way to the outflow layer. These two regions are separated by a strong

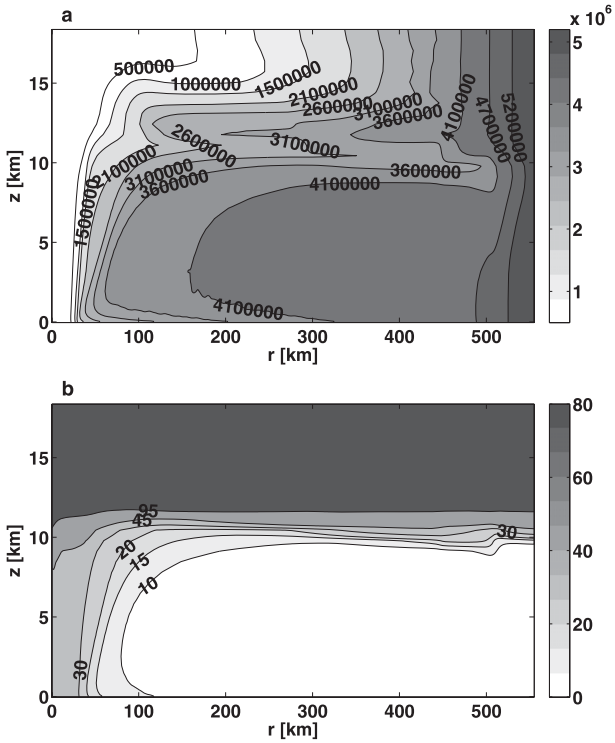

FIG. 5. For the dry simulation, cross sections of the quasi-steady-state (a) angular momentum (m^2 s^{-1}) and (b) entropy (J kg^{-1} K^{-1}) averaged over 72 h. In both plots the eyewall of the storm is quite distinguishable. The angular momentum is well mixed by the storm circulation and is constant at the midlevels of the hurricane.

entropy gradient in the eyewall. In a dry hurricane-like circulation the high entropy is generated during the inflow and then it is transported upward and out in the outflow. While the convection removes the stratification in the midlevels the outflow itself recreates the stratification near the tropopause.

Figure 6 shows the angular momentum and entropy field in the moist simulations. The angular momentum field (Fig. 6a) is almost uniform below the outflow. It is qualitatively similar to the dry angular momentum field, but stronger and more uniform. The moist entropy field, shown in Fig. 6b, has a fairly well-mixed eye (similar to the dry storm); however, the structure of this field outside the eyewall is entirely different from the dry case.

In the moist entropy field there are two phenomena apparent from the plot. First, we see a midlevel entropy minimum, which is typical in a moist atmosphere. The vertical moist entropy gradient can be expressed by the liquid entropy gradient and the water content (Pauluis et al. 2010):

$$\frac{\partial S}{\partial z} = \frac{\partial S_l}{\partial z} + \delta s_0 \frac{\partial q_T}{\partial z}.$$

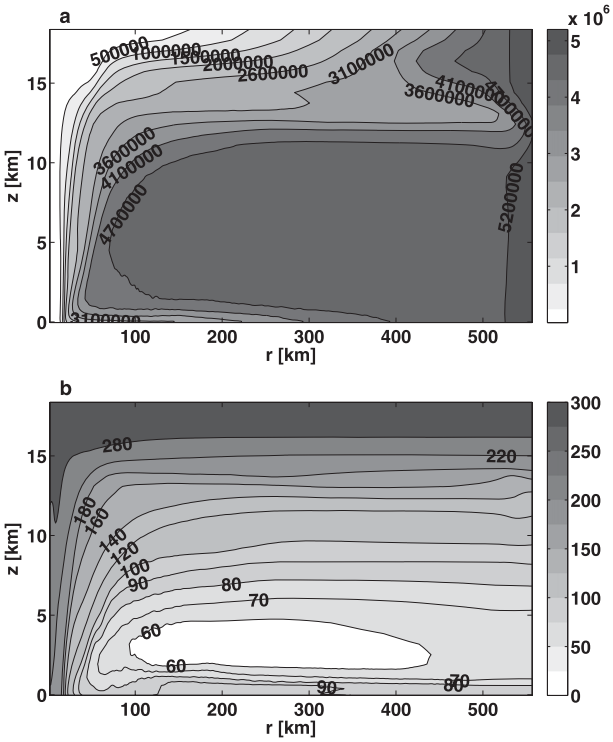

FIG. 6. (a) Quasi-steady angular momentum and (b) entropy from the moist simulation, averaged over 72 h. The angular momentum ($m^2\ s^{-1}$) field has higher values than in the dry case but is otherwise similar. The entropy field ($J\ kg^{-1}\ K^{-1}$) has a midlevel minimum and an interesting feature near 50 km where the lower entropy contour dips and touches the surface.

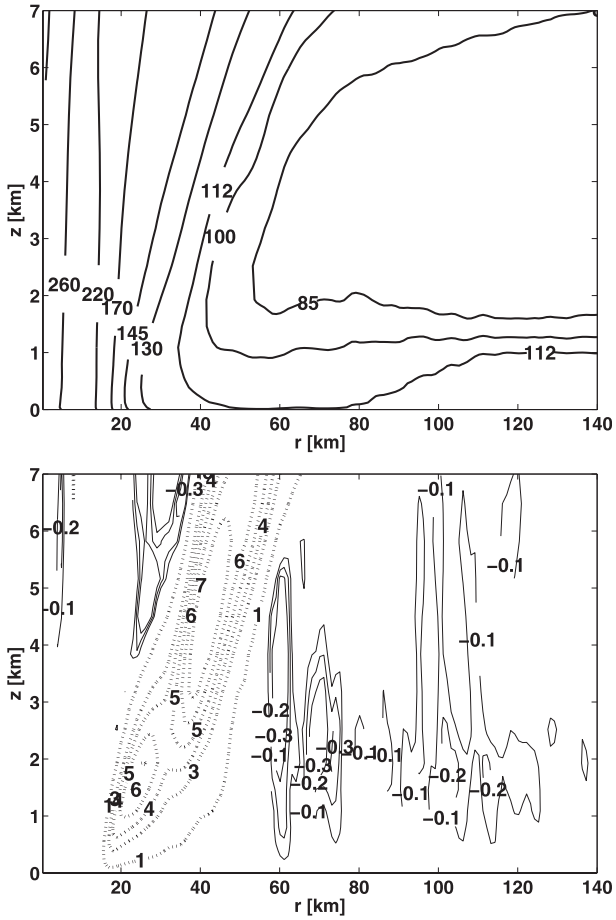

FIG. 7. Close-up view of solution in Fig. 6, showing (top) moist entropy ($J\ kg^{-1}\ K^{-1}$) and (bottom) vertical velocity ($m\ s^{-1}$). Lower-entropy surfaces are being dragged toward the surface because of the downdrafts shown in the bottom panel of this figure. The strongest downdrafts are located at around a 50–60-km radius, which corresponds well to the dip in the entropy field.

While the liquid water entropy S_l increases with height, the water content q_T drops dramatically. As shown in Pauluis et al. (2010), $\delta s_0 = (L_v/T) - r_v \log(e_0/e_S)$, where e_S is the saturation vapor pressure and e_0 is the reference partial pressure chosen to be at saturation for a reference temperature T_0. The two competing effects are the cause for the midtropospheric minimum in the entropy profile. This minimum is a signature of subsaturation in the free troposphere.

The second feature apparent in the moist entropy is a dip in the lower entropy contour at a radius of 50 km. A close-up view of the moist entropy field and vertical currents associated with it are shown in Fig. 7. The reason for this plunge in the entropy field is explained by the vertical velocity field shown in the bottom panel of Fig. 7. The strongest downdrafts of about 20–30 cm s^{-1} are at around 50–60 km, collocated with the dip in the entropy contours. These downdrafts are induced by the re-evaporation of precipitation falling from the hurricane outflow. As moisture re-evaporates, it decreases the potential temperature of the air parcel, while leaving its moist entropy unchanged (except for a small irreversible entropy production due to the evaporation of water in unsaturated air). These downdrafts result in an injection of low entropy air from the middle troposphere in the boundary and may prevent the expansion of the eyewall, as discussed in E86.

5. Qualitative sensitivity of dry hurricane intensity and size

Dry storms produced with our axisymmetric numerical model have both dynamic and thermodynamic characteristics that are similar to their moist counterparts. The primary circulation is qualitatively similar between the two regimes, but there are differences in the secondary flow, and these are directly related to the presence of water. Based on this observation we carried out a number of sensitivity tests, reported in this section.

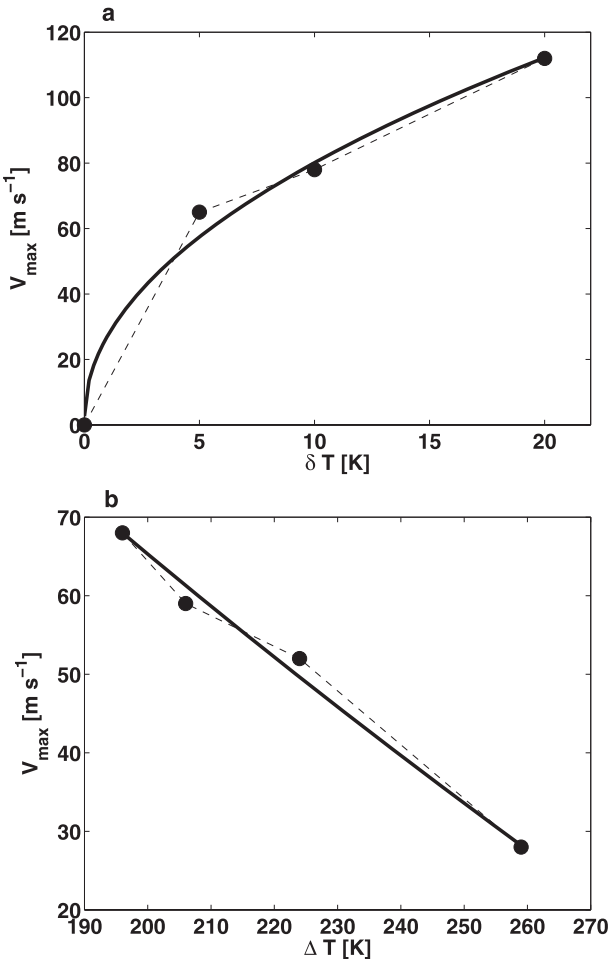

FIG. 8. (a) Sensitivity of V_{max} to ΔS, which is expressed here by the temperature difference δT between the atmosphere near the surface and the surface itself (data points). The larger the difference, the stronger the resulting storm. The solid line represents the theoretical fit. (b) Dependence of V_{max} on T_o, which is directly related to ΔT. The solid line is the theoretical fit. Here the relationship is the opposite: the warmer the tropopause temperature, the weaker the resulting storm.

These tests are qualitative for now, and a more detailed discussion of storm intensity will be covered in a following paper.

We evaluated the theoretical scaling law for the intensity of the storms. According to (2.10), V depends on two major control parameters: $V^2 \approx \Delta S \Delta T$, where ΔT is the temperature difference between the surface beneath the eyewall and the outflow, and ΔS is the entropy difference between the near-surface air and the surface itself. We use the temperature difference between the atmospheric profile in the outer regions and the ocean as a proxy for ΔS, albeit the theory would use the entropy difference at the radius of maximum wind. The results are shown in Fig. 8a. When the surface temperature is the same as the atmospheric temperature (no thermodynamic disequilibrium), the storm does not develop. For other values of the temperature jump, typically the larger the difference, the stronger the resulting storm: since the surface flux is proportional to the temperature difference, more energy is available to be converted to kinetic energy when the surface temperature is increased.

The second component of the scaling is the response of intensity to changing outflow temperature. Because the environmental temperature profile follows a dry adiabat, it is possible to achieve a different outflow temperature for the modeled storm by shifting the tropopause height. The tropopause values used here have been shifted from the level of 196 K down toward warmer values. The results are plotted in Fig. 8b. Here we find that warmer tropopause temperatures correspond to weaker storms. This is consistent with (2.10). For the warmest outflow, ΔT is smaller and the hurricane should be weaker. Both of the preliminary intensity scaling studies show agreement between modeled storms and the theoretical scaling.

Potential intensity theory does not predict the RMW, and while intensity scaling works very well for both thermodynamic setups, not much is known about what sets the RMW. As reported by, for example, Merrill (1984), observed tropical cyclones vary greatly in size, and there is no simple correlation between the RMW and other obvious dynamical parameters, such as maximum wind speed, minimum central pressure, or environmental conditions such as sea surface temperature (Gray and Shea 1973). Recently, Hill and Lackmann (2009) showed that, in numerical simulations, the RMW is related to the environmental relative humidity. In their results, higher relative humidity resulted in a larger RMW. In addition it has been observed (Kimball and Mulekar 2004) that a tropical cyclone's RMW tends to contract as the storm intensifies.

Figure 9 shows the RMW against the maximum tangential wind, for all the cases run with a range of initial and environmental conditions (surface temperature, outflow temperature, latitude, environmental profiles, etc.) in a 550-km domain. The RMW relationship to the maximum intensity is very different for the dry and moist storms. The dry cases appear to follow an angular momentum–conserving law of the form

$$V = \frac{a}{r} + br. \tag{5.1}$$

Solving (2.1) for V, the parameter a corresponds to the angular momentum, and $-2b$ is an effective Coriolis parameter. A regression fit of the dry storms (excluding

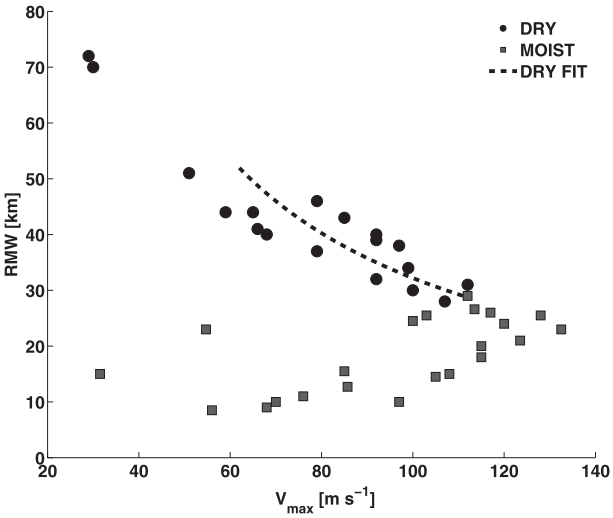

FIG. 9. Quasi-steady V_{max} vs RMW, averaged over 48–72 h. Dry storms are marked with circles and moist vortices are marked with squares. The dashed line shows the angular momentum–conserving solution.

the two weakest storms) returns $a = 3.22 \times 10^6$ m s^{-1} and $b = -4.5 \times 10^{-5}$ s^{-1}. The fitted value for a corresponds closely to the value of the angular momentum for a stationary parcel at $r = 410$ km, not far from the outer wall of the simulated domain. The effective Coriolis parameter, however, is about twice as large as the actual Coriolis parameter [$f(15°) = 3.7 \times 10^{-5}$ s^{-1}], though the sensitivity of the velocity to this parameter is small given the range of RMW here. In the moist case, the RMW shows a small increase with V_{max}, which contrasts with the inverse relationship between RMW and maximum wind in the dry case.

The behavior of the dry storms is consistent with a constant angular momentum inflow from the outer regions, but the moist storms behave differently. The different relationships between RMW and maximum wind speed for the dry and moist runs most likely indicate that moist processes play a key role in determining the RMW for hurricanes in the earth's atmosphere. A possible explanation lies in the role of the precipitation-induced downdrafts in the moist simulations, which, by entraining low entropy air into the boundary layer, may prevent the expansion of the eyewall.

6. Discussion and conclusions

In this paper we have shown that a steady hurricane-like vortex can develop in a dry atmosphere (i.e., in the absence of water vapor and phase transition). The possibility of dry hurricanes is implicit in the theory of E86, and this theoretical prediction was validated here with a series of high-resolution, axisymmetric simulations. The existence of stable, steady-state dry hurricane solutions in our numerical model confirms that hurricanes are driven by the energy transfer from the surface, and that latent heat release in the eyewall is not necessary. Moreover, simulated dry and moist storms have a similar primary circulation and somewhat similar secondary circulation.

While dry and moist hurricanes share many similar features, our simulations also show notable differences. First, the strong inflow in a dry hurricane is significantly deeper than in comparable moist storms. Second, in the moist simulations, we observed the presence of precipitation-induced downdrafts outside the eyewall, associated with the injection of low-entropy air in the boundary layer. This feature is completely absent in the dry storm. Finally, we noted a different relationship between the radius of maximum wind and the maximum wind speed. We suspect that the contrast in these relationships is tied to the difference between dry and moist thermodynamics, and, in particular, to the absence of a midtropospheric minimum of entropy and re-evaporation of precipitation in a dry atmosphere.

The fact that hurricane-like vortices can be maintained even in the absence of water vapor suggests that hurricanes could develop even during cold climates. The PI theory does not offer any theoretical lower bound on the surface temperature at which hurricanes can form, as long as the atmosphere is close to radiative–convective equilibrium. The ice age atmosphere was both colder and drier than the present-day conditions, but even such a presumably hurricane-adverse atmosphere had the potential to support the development of tropical cyclones (Hobgood and Cerveny 1988). As reported by Scileppi and Donnelly (2007), several major hurricanes occurred near the western end of Long Island during the latter part of the Little Ice Age (~1550–1850). The authors used the storm-induced deposits preserved in the coastal sedimentary layers to extend the record of landfalling hurricanes beyond historical observations. According to paleoclimate estimates cited in Scileppi and Donnelly (2007), SSTs were cooler by 2 K in the Caribbean region and by 1 K both in the Florida Keys and the Bermuda Rise.

There are also examples of hurricane-like vortices, sustained by surface disequilibrium, outside the tropics. One such example could be the polar low, which is a relatively small (less than 1000 km) but intense storm that occurs during winter over arctic oceans, poleward of the main polar fronts (Rasmussen and Turner 2003). These cyclonic storms form when a deep mass of cold air flows over warm water, creating a large air–sea disequilibrium. Most of the total entropy difference between the ocean and atmosphere in the case of polar

lows results from the large temperature difference between the two fluids rather than from the subsaturation of the air at the surface (Emanuel 1988b). In extreme cases, they have hurricane-strength winds and bring significant precipitation.

Another interesting example of hurricane-like vortices is ''medicanes,'' the large cyclonic storms that develop over the Mediterranean Sea. Observations show (Fita et al. 2007) that these have near-hurricane magnitude and structure but tend to live only 2–3 days, probably because of the smaller size of the sea basin compared to the Atlantic Ocean. As reported by Fita et al. (2007), the Mediterranean storms exist in an environment that differs from typical tropical conditions. They develop in winter, when the sea surface temperature is much lower than the value of 299 K (26°C) that is commonly cited as the threshold temperature for hurricane development. The environmental profile of these Mediterranean hurricanes shows intrusions of dry African air and some colder air in midtropospheric levels, when compared to the typical tropical sounding.

Our study confirms that hurricanes result from the thermodynamic disequilibrium between the atmosphere and ocean, and that their intensity is primarily controlled by the entropy and angular momentum fluxes from the surface. In the tropical atmosphere, high entropy is achieved through the addition of water vapor. However, in a drier atmosphere, an increase of entropy from sensible heating can play a similar role in sustaining hurricane-like vortices. A manuscript is in preparation to further analyze the energy and momentum budget of the boundary layer by comparing the dry and moist storms. While water vapor and phase transitions are an intrinsic part of tropical storm, dry hurricanes provide a simplified framework to study hurricane intensity and can offer new insights by pointing out whether specific aspects of hurricanes are directly affected by moist processes.

Acknowledgments. We thank Kerry Emanuel and two anonymous reviewers for comments that helped to improve this manuscript. The simulations were performed on the GFDL High Performance Computing system. AM thanks her current employers, Columbia University and NASA/GISS, for supporting her continuing work on this subject. This work was partially supported by the NSF Grant ATM-0545047.

REFERENCES

Anderson, J. L., and Coauthors, 2004: The new GFDL global atmosphere and land model AM2-LM2: Evaluation with prescribed SST simulations. *J. Climate,* **17,** 4641–4673.

Beljaars, A. C. M., 1994: The parametrization of surface fluxes in large-scale models under free convection. *Quart. J. Roy. Meteor. Soc.,* **121,** 255–270.

Clough, S. A., M. J. Iacono, and J. Moncet, 1992: Line-by-line calculations for atmospheric fluxes and cooling rates: Application to water vapor. *J. Geophys. Res.,* **97,** 15 761–15 785.

Emanuel, K. A., 1986: An air–sea interaction theory for tropical cyclones. Part I: Steady-state maintenance. *J. Atmos. Sci.,* **43,** 585–604.

——, 1988a: The maximum intensity of hurricanes. *J. Atmos. Sci.,* **45,** 1143–1155.

——, 1988b: Toward a general theory of hurricanes. *Amer. Sci.,* **76,** 370–379.

——, 1995: Sensitivity of tropical cyclones to surface exchange coefficients and a revised steady-state model incorporating eye dynamics. *J. Atmos. Sci.,* **52,** 3969–3976.

——, 1997: Some aspects of hurricane inner-core dynamics and energetics. *J. Atmos. Sci.,* **54,** 1014–1026.

Fita, L., R. Romero, A. Luque, K. Emanuel, and C. Ramis, 2007: Analysis of the environments of seven Mediterranean tropical-like storms using an axisymmetric, nonhydrostatic, cloud resolving model. *Nat. Hazards Earth Syst. Sci.,* **7,** 41–56.

Freidenreich, S. M., and V. Ramaswamy, 1999: A new multiple-band solar radiative parametrization for general circulation models. *J. Geophys. Res.,* **104,** 31 389–31 409.

Garatt, J. R., 1992: *The Atmospheric Boundary Layer*. Cambridge University Press, 316 pp.

Gray, W., 1968: Global view of the origin of tropical disturbances and storms. *Mon. Wea. Rev.,* **96,** 669–700.

——, and D. Shea, 1973: The hurricane's inner core region. II: Thermal stability and dynamic characteristics. *J. Atmos. Sci.,* **30,** 1565–1576.

Hill, K. A., and G. M. Lackmann, 2009: Influence of environmental humidity on tropical cyclone size. *Mon. Wea. Rev.,* **137,** 3294–3315.

Hobgood, J. S., and R. S. Cerveny, 1988: Ice-age hurricanes and tropical storms. *Nature,* **333,** 243–245.

Holland, G. J., 1997: The maximum potential intensity of tropical cyclones. *J. Atmos. Sci.,* **54,** 2519–2541.

Jordan, C., 1958: Mean sounding for the West Indies area. *J. Meteor.,* **15,** 91–97.

Kimball, S., and M. Mulekar, 2004: A 15-year climatology of North Atlantic tropical cyclones. Part I: Size parameters. *J. Climate,* **17,** 3555–3575.

Kleinschmidt, E., 1951: Grundlagen einer Theorie der tropischen Zyklonen (Principles of the theory of tropical cyclones). *Arch. Meteor. Geophys. Bioklimatol.,* **4A,** 53–72.

Klemp, J., and R. Wilhelmson, 1978: The simulation of three-dimensional convective storm dynamics. *J. Atmos. Sci.,* **35,** 1070–1096.

Krueger, S. K., Q. Fu, K. N. Liou, and H.-N. S. Chin, 1995: Improvements of an ice-phase microphysics parameterization for use in numerical simulations of tropical convection. *J. Appl. Meteor.,* **34,** 281–287.

Lin, Y.-L., R. Farley, and H. Orville, 1983: Bulk parameterization of the snow field in a cloud model. *J. Appl. Meteor.,* **22,** 1065–1092.

Lord, S. J., H. E. Willoughby, and J. M. Piotrowicz, 1984: Role of a parameterized ice-phase microphysics in an axisymmetric, nonhydrostatic tropical cyclone model. *J. Atmos. Sci.,* **41,** 2836–2848.

Malkus, J. S., 1958: On the structure and maintenance of the mature hurricane eye. *J. Meteor.,* **15,** 337–349.

——, and H. Riehl, 1960: On the dynamics and energy transformations in steady-state hurricanes. *Tellus,* **12,** 1–20.

Merrill, R. T., 1984: A comparison of large and small tropical cyclones. *Mon. Wea. Rev.,* **112,** 1408–1418.

Miller, B. I., 1958: On the maximum intensity of hurricanes. *J. Meteor.,* **15,** 184–195.

Moon, I.-J., I. Ginis, T. Hara, and B. Thomas, 2006: A physics-based parameterization of air–sea momentum flux at high wind speeds and its impact on hurricane intensity predictions. *Mon. Wea. Rev.,* **135,** 2869–2878.

Pauluis, O. M., and S. T. Garner, 2006: Sensitivity of radiative convective equilibrium simulations to horizontal resolution. *J. Atmos. Sci.,* **63,** 1910–1923.

——, A. Czaja, and R. Korty, 2010: The global atmospheric circulation in moist isentropic coordinates. *J. Climate,* **23,** 3077–3093.

Pearce, R., 1998: A study of hurricane dynamics using a two-fluid axisymmetric model. *Meteor. Atmos. Phys.,* **67,** 71–81.

——, 2004: An axisymmetric model of a mature tropical cyclone incorporating azimuthal vorticity. *Quart. J. Roy. Meteor. Soc.,* **130,** 259–293.

Rasmussen, E., and J. Turner, 2003: *Polar Lows: Mesoscale Weather Systems in the Polar Regions*. Cambridge University Press, 624 pp.

Schwarzkopf, M. D., and V. Ramaswamy, 1999: Radiative effects of CH_4, N_2O, halocarbons and the foreign-broadened H_2O continuum: A GCM experiment. *J. Geophys. Res.,* **104,** 9467–9488.

Scileppi, E., and J. P. Donnelly, 2007: Sedimentary evidence of hurricane strikes in western Long Island, New York. *Geochem. Geophys. Geosyst.,* **8,** Q06011, doi:10.1029/2006GC001463.

Stevens, B., 2005: Atmospheric moist convection. *Annu. Rev. Earth Planet. Sci.,* **33,** 605–643.